In conclusion, for the extreme case of delamination-prone laminates characterized here, the serration procedure of Ref. 1 has been shown to be effective in withstanding free edge delamination under static loading and resisting applied stresses comparable to laminate ultimate strength. Under sufficiently high stress levels in a fatigue environment, however, a highly undesirable (catastrophic) failure mode occurs. This indicates that tensile values of σ_z are present at the free edge in TS, however, at lower stress concentration than in T. Subsequent to precipitation of delamination under fatigue loading, stress concentrations at the internal corners of the serrations evidently dominate the fracture response. Conceivably, alteration of the serration geometry, in particular, elimination of the sharp corners, may lead to improved failure characteristics.

References

[1] Dickerson, E. O. and Lackman, L. M., "Boron-Reinforced Longerons," *Proceedings of the Conference on Fibrous Composites in Flight Vehicle Design*, AFFDL-TR-72-130, Air Force Flight Dynamics Laboratory, Wright-Patterson Air Force Base, Ohio, pp. 583–617.

[2] Pagano, N. J. and Pipes, R. B., "The Influence of Stacking Sequence on Laminate Strength," *Journal of Composite Materials*, Vol. 5, Jan. 1971, pp. 50–57.

[3] Pagano, N. J. and Pipes, R. B., "Some Observations on the Interlaminar Strength of Composite Laminates," *International Journal of Mechanical Sciences*, Vol. 15, 1973, pp. 679–688.

[4] Pagano, N. J., "On the Calculation of Interlaminar Normal Stress in Composite Laminates," *Journal of Composite Materials*, Vol. 8, Jan. 1974, pp. 89–105.

[5] Pagano, N. J. and Rybicki, E. F., "On the Significance of Effective Modulus Solutions for Fibrous Composites," *Journal of Composite Materials*, Vol. 8, July 1974, pp. 214–228.

[6] Pagano, N. J., "Exact Moduli of Anisotropic Laminates," in *Mechanics of Composite Materials*, Vol. 2, edited by G. P. Sendeckyj, Academic Press, New York, 1974, pp. 23–44.

Vibrations of Sandwich Beams with Central Masses

SHAUKAT MIRZA* AND ANAND V. SINGH†

University of Ottawa, Ottawa, Canada

Introduction

SEVERAL papers dealing with the vibration of beams having masses have been published in the past.[1-3] With the increasing use of sandwich construction in the modern technology, efforts have also been made in studying the dynamic response of layered beams, plates, and shells without any mass.[4-6]

In this Note an attempt has been made to study the natural frequencies of vibration of sandwich beams with central masses. A treatment of this type of problem is not available in the literature. The beam considered in this study is composed of isotropic thin face sheets and a thick core. The two face sheets are considered to be thin and of equal thickness h. The thickness of the core is taken as c (Fig. 1). Because of the presence of mass M, two separate cases for symmetric and antisymmetric modes have been investigated.

Basic Equations

While arriving at the differential equations, the following assumptions have been used: 1) The face sheets are completely bonded to the core and there is no slip at the interfaces; 2) The core takes bending stresses in the plane of the sandwich; 3) The thin face sheets behave as membranes; 4) The extensional rigidity of the core in the lateral direction is infinite.

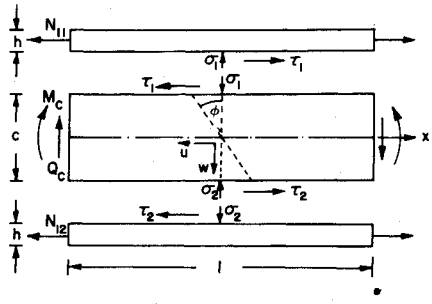

Fig. 1 Sandwich beam element showing displacements, stresses at the interfaces and on the cross-section.

The last assumption leads to the incompressibility condition of the core. The following relation is then easily established: $w_c = w_1 = w_2 = w$. The quantity w denotes the lateral deflection and the subscripts c, 1 and 2 refer to the core, the first and second face sheets, respectively. In writing the differential equations of motion, the rotary inertia of the face sheets and the core about the middle plane is neglected. This is a valid assumption, as we are concerned with the frequencies which are much below the first thickness shear frequency of the sandwich beam.

Writing the equations of motion for the core, the first and second face sheets, and eliminating the unknown interface stresses σ_1, σ_2, τ_1, and τ_2 by combining these equations, yields the following two equations,[4]

$$\begin{aligned} B\,\partial^2\phi/\partial x^2 - G_c A_c(\phi + \partial w/\partial x) &= 0 \\ G_c A_c(\partial\phi/\partial x + \partial^2 w/\partial x^2) &= m\,\partial^2 w/\partial t^2 \end{aligned} \tag{1}$$

The rotation of the transverse plane of the core and its cross sectional area are given by ϕ and A_c, respectively. Further, the shear modulus and the density of the materials of the core are represented by G_c and ρ_c. Since the present investigation deals with the free vibrations, Eqs. (1) do not contain the external loading terms. For convenience the following symbols have been introduced in Eqs. (1) and elsewhere in this Note

$$B = \tfrac{1}{2}EA_f c^2 + E_c I_c$$
$$m = \rho_c A_c[1 + 2\rho h/(\rho_c c)]; \quad K = G_c A_c$$

The modulus of elasticity and the density of the face sheets are given by E and ρ. The quantity A_f represents the cross-sectional area of a face sheet. The governing differential equation can be obtained by combining Eqs. (1) which yields the equation in terms of deflection w.

$$\partial^4 w/\partial x^4 - (m/K)\,\partial^4 w/\partial x^2\,\partial t^2 + (m/B)\,\partial^2 w/\partial t^2 = 0 \tag{2}$$

Symmetric and Antisymmetric Modes

The mass M which has a moment of inertia I^* is placed at the mid-span of the beam. The first part of the Note deals with the analysis of the symmetric modes and the later section with asymmetric modes. Two cases of simple-simple and fixed-fixed support conditions have been considered in each of these two sections. Because of the presence of the mass M, it is necessary to write these conditions separately for symmetric and nonsymmetric modes.

The normal mode solution of Eq. (2) in terms of the two variables w and ϕ is given in the form,

$$\begin{aligned} w(x,t) &= \sum W_n(x)\sin(\Omega_n t) \\ \phi(x,t) &= \sum \Phi_n(x)\sin(\Omega_n t) \end{aligned} \tag{3}$$

This separation of variables technique yields a pair of ordinary differential equations. The differential equations in the spatial variable are then solved. The solution is of the form

Received July 1, 1974; revision received August 26, 1974.

Index categories: Structural Dynamic Analysis; Aircraft Vibration.

* Associate Professor, Department of Mechanical Engineering.

† Research Assistant, Department of Mechanical Engineering.

$$W_n(x) = A_n \cos \alpha_n x + B_n \sin \alpha_n x + C_n \cosh \beta_n x + D_n \sinh \beta_n x$$

$$\Phi_n(x) = [\alpha_n - m\Omega_n^2/(G_c A_c \alpha_n)]\{A_n \sin \alpha_n x - B_n \cos \alpha_n x\} - [\beta_n + m\Omega_n^2/(G_c A_c \beta_n)]\{C_n \sinh \beta_n x + D_n \cosh \beta_n x\} \quad (4)$$

The coefficients α_n and β_n are given as,

$$\alpha_n, \beta_n = \{\pm \tfrac{1}{2} m\Omega_n^2/K + [(\tfrac{1}{2} m\Omega_n^2/K)^2 + m\Omega_n^2/B]^{1/2}\}^{1/2} \quad (5)$$

The constants $A_n, \ldots, D_n$ are evaluated by making use of the boundary conditions.

Symmetric Modes

Two cases of simple-simple and fixed-fixed conditions have been considered in this Note.

Case 1): Simple support conditions

$$w = 0 \quad \text{and} \quad \partial\phi/\partial x = 0 \quad \text{at} \quad x = 0$$
$$\phi = 0 \quad \text{and} \quad G_c A_c(\phi + \partial w/\partial x) = -\tfrac{1}{2} M \partial^2 w/\partial t^2 \quad \text{at} \quad x = l/2 \quad (6a)$$

Case 2): Fixed end conditions

$$w = 0 \quad \text{and} \quad \phi = 0 \quad \text{at} \quad x = 0$$
$$\phi = 0 \quad \text{and} \quad G_c A_c(\phi + \partial w/\partial x) = -\tfrac{1}{2} M \partial^2 w/\partial t^2 \quad \text{at} \quad x = l/2 \quad (6b)$$

Asymmetric Modes

For these modes the dynamic conditions of the beam and the mass are modified. These will again be listed for the two support conditions.

Case 1): Simple support conditions

$$w = 0 \quad \text{and} \quad \partial\phi/\partial x = 0 \quad \text{at} \quad x = 0$$
$$w = 0 \quad \text{and} \quad -EI(\partial^2 w/\partial x^2) = \tfrac{1}{2} I^* \partial^2 \phi/\partial t^2 \quad \text{at} \quad x = l/2 \quad (7a)$$

Case 2): Fixed end conditions

$$w = 0 \quad \text{and} \quad \phi = 0 \quad \text{at} \quad x = 0$$
$$w = 0 \quad \text{and} \quad -EI\,\partial^2 w/\partial x^2 = \tfrac{1}{2} I^* \partial^2 \phi/\partial t^2 \quad \text{at} \quad x = l/2 \quad (7b)$$

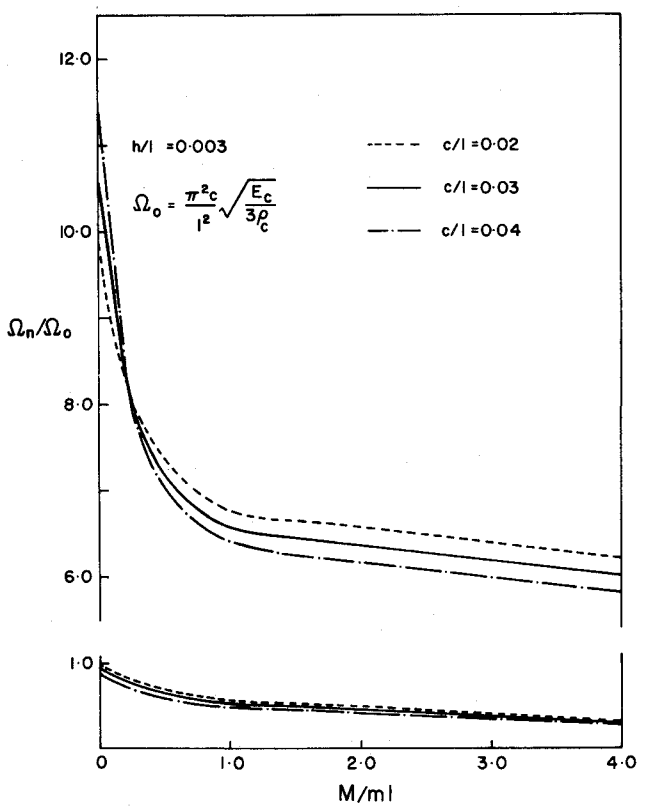

Fig. 2 Variation of nondimensional frequency parameter Ω_n/Ω_0 against the mass ratio M/ml for a simply supported beam.

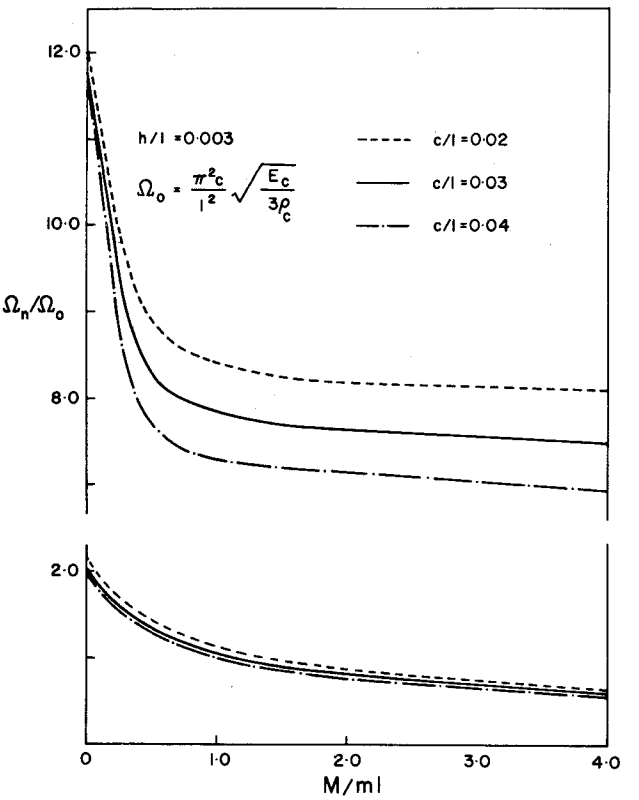

Fig. 3 Variation of nondimensional frequency parameter Ω_n/Ω_0 against the mass ratio M/ml for a fixed ended beam.

The application of these conditions (6a) and (6b) will yield the following set of equations for symmetric modes.

Case 1):

$$A_n + C_n = 0 \quad (8a)$$

$$A_n \alpha_n K_1 - C_n \beta_n K_2 = 0 \quad (8b)$$

$$K_1 l[A_n \sin(\alpha_n l/2) - B_n \cos(\alpha_n l/2)] - K_2 l[C_n \sinh(\beta_n l/2) + D_n \cosh(\beta_n l/2)] = 0 \quad (8c)$$

$$A_n[G_c A_c(K_1 - \alpha_n)\sin(\alpha_n l/2) - \tfrac{1}{2} M\Omega_n^2 \cos(\alpha_n l/2)] + B_n[G_c A_c(-K_1 + \alpha_n)\cos(\alpha_n l/2) - \tfrac{1}{2} M\Omega_n^2 \sin(\alpha_n l/2)] + C_n[G_c A_c(-K_2 + \beta_n)\sinh(\beta_n l/2) - \tfrac{1}{2} M\Omega_n^2 \cosh(\beta_n l/2)] + D_n[G_c A_c(-K_2 + \beta_n)\cosh(\beta_n l/2) - \tfrac{1}{2} M\Omega_n^2 \sinh(\beta_n l/2)] = 0 \quad (8d)$$

Case 2): For this case Eqs. (8a), (8c) and (8d) are the same and Eq. (8b) is replaced by Eq. (9).

$$-B_n K_1 l - D_n K_2 l = 0 \quad (9)$$

Further, the asymmetric vibration of the beam will lead to the following equations.

Case 1): It can be seen that Eqs. (8a) and (8b) are applicable while the last two conditions in (7a) yield,

$$A_n \cos(\alpha_n l/2) + B_n \sin(\alpha_n l/2) + C_n \cosh(\beta_n l/2) + D_n \sin(\beta_n l/2) = 0 \quad (10a)$$

$$A_n[2EI/(lI^*)(\alpha_n l)^2 \cos(\alpha_n l/2) + \Omega_n^2 K_1 l \sin(\alpha_n l/2)] + B_n[2EI/(lI^*)(\alpha_n l)^2 \sin(\alpha_n l/2) - \Omega_n^2 K_1 l \cos(\alpha_n l/2)] - C_n[2EI/(lI^*)(\beta_n l/2)^2 + \Omega_n^2 K_n l \sinh(\beta_n l/2)] - D_n[2EI/(lI^*)(\beta_n l)^2 \sinh(\beta_n l/2) + \Omega_n^2 K_2 l \cosh(\beta_n l/2)] = 0 \quad (10b)$$

Case 2): Here, Eq. (8a) is still applicable, while the last two equations are the same as Eqs. (10). However, Eq. (8b) takes the form,

$$K_1 l B_n + K_2 l D_n = 0 \quad (11)$$

The use of these conditions yields the transcendental frequency equation,

$$|a_{ij}| = 0 \qquad i,j = 1,\ldots,4 \tag{12}$$

The frequency Eq. (12) is written separately for the two cases depending on symmetric or anti-symmetric mode condition.

Numerical Computations and Results

Computations were carried out for the symmetric modes and for the two types of end conditions mentioned in Cases 1 and 2. The ratio of the density of the face sheet material to that of the honeycomb core r_ρ is assumed to be 1/21. The ratio of moduli of rigidity of the face sheet to the core is taken as 30 for all calculations. Poisson's ratio of all the layers is assumed to be equal and of magnitude 0.3. Computations were carried out for three values of h/l which are 0.001, 0.003, and 0.005 and for four different values of c/l ranging from 0.01 to 0.04 at interval of 0.01. The frequencies were generated for first three symmetric modes by varying the ratio M/ml from zero to 4.0. Some of these results are shown in Figs. 2 and 3. These figures show the variation of Ω_n/Ω_0 against the mass ratio M/ml for two modes. The plot in Fig. 2 is for a simply supported beam while that in Fig. 3 is for fixed ended beam.

References

1 Baker, W. E., "Vibration Frequencies for Uniform Beams with Central Masses," *Transactions of the ASME; Journal of Applied Mechanics*, Vol. 31, Ser. E, June 1964, pp. 335–337.

[2] Chen, Yu, "On the Vibration of Beams or Rods Carrying a Central Mass," *Transactions of the ASME; Journal of Applied Mechanics*, Ser E: Vol. 30, June 1963, pp. 310–311.

[3] Hess, M. S., "Vibration Frequencies of a Uniform Beam with Central Mass and Elastic Supports," *Transactions of the ASME: Journal of Applied Mechanics*, Ser. E, Vol. 31, Sept. 1964, pp. 556–558.

[4] Nicholas, T. and Heller, L. A., "Determination of the Complex Shear Modulus of a Filled Elastomer From a Vibrating Sandwich Beam," *Experimental Mechanics*, March 1967, pp. 110–116.

[5] Raville, M. E., Ueng, C. E. S., and Lei, M. M., "Natural Frequencies of Vibration of Fixed-Fixed Sandwich Beams," *Transactions of the ASME: Journal of Applied Mechanics*, Vol. 28, Sept. 1961, pp. 367–371.

[6] Yu, Y. Y., "Flexural Vibrations of Elastic Sandwich Plates," *Journal of Aero-space Sciences*, Vol. 27, No. 4, April 1960, pp. 272–282.

Attainment of Jupiter Entry Shock Velocities

LEWIS P. LEIBOWITZ*
Jet Propulsion Laboratory, Pasadena, Calif.

Introduction

EFFORTS to develop shock tubes that simulate entry of a probe into the atmosphere of Jupiter have been under way for several years. Progress towards these goals has been described by Menard,[1] Dannenberg,[2] Livingston and Menard,[3] and Compton and Cooper.[4] The conical arc driver[1-3] has increased the attainable shock speed with 1.0 torr initial pressure from 15 to 34 km/sec and has allowed the simulation of some of the variables for Jupiter entry; for example, the temperature. Yet, performance has fallen short of the goal of 40 km/sec shock velocities in hydrogen-helium mixtures with initial pressures of 1.0 torr or greater. The Voitenko compressor driven shock tube[4] produced shock waves at greater than Jupiter entry velocity, but was unsuitable for sustained investigation because it destroyed itself during each firing. With the annular arc accelerator (ANAA) shock tube, 47 km/sec shock velocities have been achieved in 1.0 torr of hydrogen.

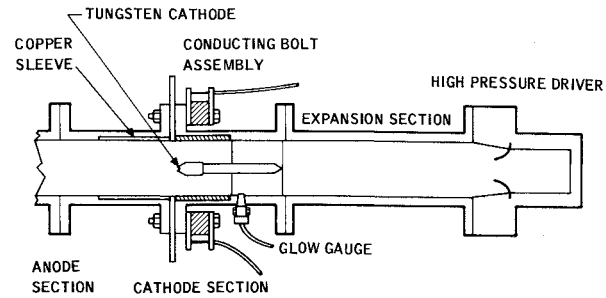

Fig. 1 Schematic diagram of the ANAA driver.

The ANAA consists of a cold gas driver, an expansion section, the electrode sections and the shock tube test section (see Fig. 1). A high pressure cold gas driver is used to flow a stream of gas past a high voltage electrode section. The driver gas accelerates into the expansion section driving a shock wave in front of it. As the flowing gas passes through the electrode sections, the energy of a high-voltage capacitor bank is discharged into the gas. The arc heated plasma immediately expands and cools, driving a shock wave down the tube. This immediate expansion greatly reduces the opportunity for the gas to lose energy by radiative cooling during the diaphragm opening process.

The initial operating experience of the ANAA shock tube has been previously described.[5] In the initial configuration, the capacitor bank lacked a switching capability and an auxiliary insulating diaphragm was placed between the electrode sections of the ANAA to act as a passive switch. However, the slow breaking of the insulating diaphragm disrupted the driver gas flow and prevented the ANAA from reaching its full potential.

Design

The ANAA driver is designed to coordinate the flow from a high pressure helium driver with the discharge from one hundred 20 KV capacitors. The capacitor bank is controlled by a high-voltage discharge system consisting of a flow detector, trigger generator, and a high-current switching system. Flow is initiated in the 15 cm diam electrode sections by bursting a scribed brass diaphragm with helium at a pressure of approximately 1500 psi. A shock wave followed by the driver gas then passes through the cathode section. The current is transferred to the gas through a pointed tungsten alloy cathode that is attached to an aluminum shaft. The aluminum anode section has a press-fit copper sleeve that absorbs the discharge current.

The ANAA driver switching system is capable of discharging over 1 million amp currents into the driver gas. The capacitor discharge trigger system includes a glow gage transducer to sense the arrival of the driver gas at the electrode section, a pulse forming circuit, a delay generator, a high voltage spark generator, and four spark gaps. The system is described in more detail elsewhere.[6,7]

Results

The effect on ANAA performance of variations in capacitor bank voltage, and the compositions and pressures of the driver and test gases has been investigated. The most significant variations in shock speed were produced by varying the test gas composition and the capacitor bank energy. In Fig. 2, a plot is shown of the shock velocity 8.3 m from the arc as a function of capacitor bank energy for several test gases. Velocities up to

Submitted June 26, 1974; presented as Paper 74-610 at the AIAA 8th Aerodynamic Testing Conference, Bethesda, Md., July 8–10, 1974; revision received September 23, 1974. This research sponsored by NASA under Contract NAS7-100.

Index category: Shock Waves and Detonations, Entry Vehicle Testing.

* Member of the Technical Staff.